VOL. 19, NO. 17, SEPTEMBER 2024 ISSN 1819-6608
ARPN Journal of Engineering and Applied Sciences

www.arpnjournals.com

THE EFFECT OF CORRELATED COLOR TEMPERATURE (CCT) VARIATION ON SPECTRAL MISMATCH FACTOR (SMF) FOR INCANDESCENT LUMINOUS FLUX LAMPS

Manal A. Haridy
Photometry and Radiometry Division, National Institute of Standards (NIS), Giza, Egypt
E-Mail: manal_haridi@yahoo.com

ABSTRACT

This work employed an experimental setup, consisting of an NIS Spectroradiometer from Ocean Optics HR 2000 with a measurement uncertainty of 4.7%, a photometric bench, and a series of NIS total luminous flux standard lamps previously calibrated at the National Physical Laboratory in England with an uncertainty of 0.8%. The following setup allowed the measurement of the correlated color temperature and spectral power distribution for six incandescent lamps. The most important basis for assessing the uncertainty and variations that occur in the spectral mismatch correction factor for each of the lamps is the CCT curves and their formula. Uncertainty calculations were therefore done to further investigate the lamp behavior and it was found that the CCT for the standard lamps must be in the interval starting from 2400 K up to 2750 K. For the tested lamps, CCT must lie between 2043 K and 2095 K. This spread in CCT highly affects the uncertainty of SMF. A very intensive analysis of the data led to an uncertainty model that followed the measurement results. The developed model was important in estimating the uncertainties associated with the SMF, which was about 0.0011 to 0.0084, depending on the CCT of the lamps. The correlation between CCT and SMF shows the importance of accurate calibration and good uncertainty modeling in photometric measurements.

Keywords: the correlated color temperature (CCT), the spectral mismatch correction factor (SMF), Incandescent lamps, uncertainty analysis.

Manuscript Received 4 July 2024; Revised 30 September 2024; Published 10 December 2024

1. INTRODUCTION

A shift in Correlated Color Temperature (CCT) signifies an alteration in the spectral power distribution and consequently the irradiance. By measuring CCT, rather than conducting a spectral analysis, one can detect changes in the source irradiance, which subsequently affects photovoltaic testing outcomes [1]. Performances evaluation of the whole PV system, researchers are putting huge effort into incident solar irradiance measurement. That is where SPD and CCT of the incoming light provide the necessary characteristics. The color temperature of a Planckian black body radiator in degrees Kelvin is a measure of its spectral power distribution. The spectral power distribution is a detailed description of the way in which the power is distributed across different wavelengths of light. This relation of SPD with the color temperature gives insight into the spectral qualities of the irradiance. Another critical metric is the Correlated Color Temperature, which represents the color temperature closest to the idealized Planckian black body radiator. This relationship is described by the Planckian curve, Tc (K), as illustrated in Figure 1. CCT reduces the light quality characteristic to a single number that describes whether the light "color temperature" is "cool" or "warm." A "cool" light source, such as a clear blue sky, can have a CCT of as much as 12000 K, while a "warm" light source, such as a red sunset, could have a CCT of around 2000 K. Computation of the CCT includes integration over relevant wavelengths of the SPD of the incident light with the CIE spectral tristimulus values $\bar{x}(\lambda)$, $\bar{y}(\lambda)$, and $\bar{z}(\lambda)$. The tristimulus values of $\bar{x}$, $\bar{y}$, and $\bar{z}$ form the very basis of color science, based on experimental work performed in 1931 that studied human color perception. In these experiments subjects viewed various quantities of red, green, and blue light all within a 2° field of view and provided the data for the $\bar{x}(\lambda)$, $\bar{y}(\lambda)$, and $\bar{z}(\lambda)$ functions that describe the quantity at various wavelengths that activates the red, green, and blue photoreceptors within the human eye.

From this data the X(T), Y(T) and Z(T) color matching functions are computed using equations (1), (2) and (3) respectively where L is the incident sunlight. The aforementioned functions serve to quantify how the SPD of a light source relates to human color perception and, therefore, enable determination of CCT. Calculations regarding CCT must be made as exact as possible since knowledge of performance under variant lighting conditions depends on these data; primarily, changes in CCT may alter the efficiency with which solar panels convert sunlight into energy. Therefore, both SPD and CCT should be taken into consideration for realistic ambient PV performance optimizations [2, 3].

$$X(T) = \int_0^\infty \bar{x}(\lambda)\, L_\lambda(\lambda, T)\, d\lambda \tag{1}$$

$$Y(T) = \int_0^\infty \bar{y}(\lambda)\, L_\lambda(\lambda, T)\, d\lambda \tag{2}$$

$$Z(T) = \int_0^\infty \bar{z}(\lambda)\, L_\lambda(\lambda, T)\, d\lambda \tag{3}$$

The CIE 1931 chromaticity equations are essential for converting the color-matching functions

X(T), Y(T), and Z(T) into chromaticity coordinates, which provide a more intuitive representation of color. These equations, represented by equations (4) and (5), calculate the x and y chromaticity coordinates. These coordinates map the perceived color of light onto a two-dimensional chromaticity diagram, which is widely used to visualize color properties. The chromaticity diagram is an important tool in color science as it shows the relationship between different colors perceived by the human eye. The x and y coordinates are calculated using the following equations:

$$x(T) = \frac{X(T)}{(X(T)+Y(T)+Z(T))} \quad (4)$$

$$y(T) = \frac{Y(T)}{(X(T)+Y(T)+Z(T))} \quad (5)$$

The Correlated Color Temperature CCT is the intersecting point between x and y values on the CIE 1931 Chromaticity Diagram, showing the light's appearance- from warm at lower temperatures to cool at higher temperatures. This point of intersection is compared to the Planckian locus or color of light emitted by a blackbody radiator at various temperatures. The lines of equal temperature, which are at right angles to the Planckian locus, help interpolate the CCT; this also can be done when the light source is not an ideal blackbody. For proper CCT determination, if required in lighting analysis, there is an absolute necessity for the CIE 1931 diagram.

$$n = \frac{(n-0.3320)}{(y-0.1858)} \quad (6)$$

$$CCT = 437n^3 + 360n^2 + 6861n - 5514.3 \quad (7)$$

The spectral power distribution SPDs are usually sampled at discrete intervals in color science and the continuous integration is replaced by summation. The tristimulus values are calculated via integration equations in a continuous wavelength range, but those adapted to summation formulae for use in practice when discrete data are being handled. That wavelength range now being applied, from 380 to 780 nm, to sampled data points, and the accuracy of this summation depends on the resolution of the sampling. Advantages: the efficient colorimetric analyses using real-world data have been enabled and become summation Equations 8, 9, and 10.

$$X = \sum_{360}^{830} \bar{x}_i\, L_i \Delta\lambda \quad (8)$$

$$Y = \sum_{360}^{830} \bar{y}_i\, L_i \Delta\lambda \quad (9)$$

$$Z = \sum_{360}^{830} \bar{z}_i\, L_i \Delta\lambda \quad (10)$$

The example CIE 1931 2° tristimulus values (x, y, and z) given here for the wavelength range from 360 nm to 830 nm in 1 nm steps show how human color perception changes with different light wavelengths.

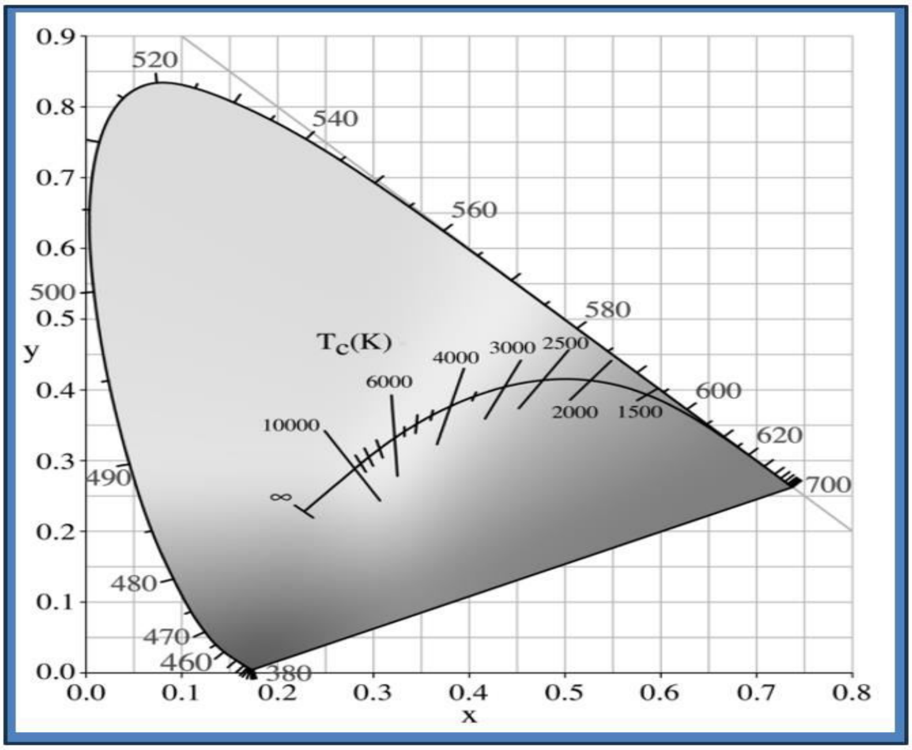

Figure-1. The 1931 CIE chromaticity diagram featuring the Planckian locus. [5]

The tristimulus values are tabulated from the spectral sensitivity of the standard observer. The x values increase for longer wavelengths, peaking in the green region, while y values peak in the green-yellow region,

ARPN Journal of Engineering and Applied Sciences

showing where the eye is most sensitive. Z values rise more gradually, reflecting sensitivity to blue wavelengths. It becomes useful in research and practice in the design of lighting, colorimetry, and displays since it gives an idea of which wavelengths correspond to which perceived colors. [4]. A more accurate determination of CCT could be done with McCamy's formulae, which give a very simplified, yet reliable approximation, starting from the chromaticity coordinates x, y and z obtained from the CIE 1931 chromaticity diagram [6]. The formula by McCamy allows an easy estimate of CCT without complicated iterative calculations, obtaining an approximate value good enough in practice for daylight or sunlight-type sources. This is very effective in representing a wide gamut of light sources, in situations where the direct integration approach may be less convenient. While the McCamy sunlight model is built with normal daylight conditions in mind, its CCT falls within the range of approximately 4800 K to 10000K[7,8].

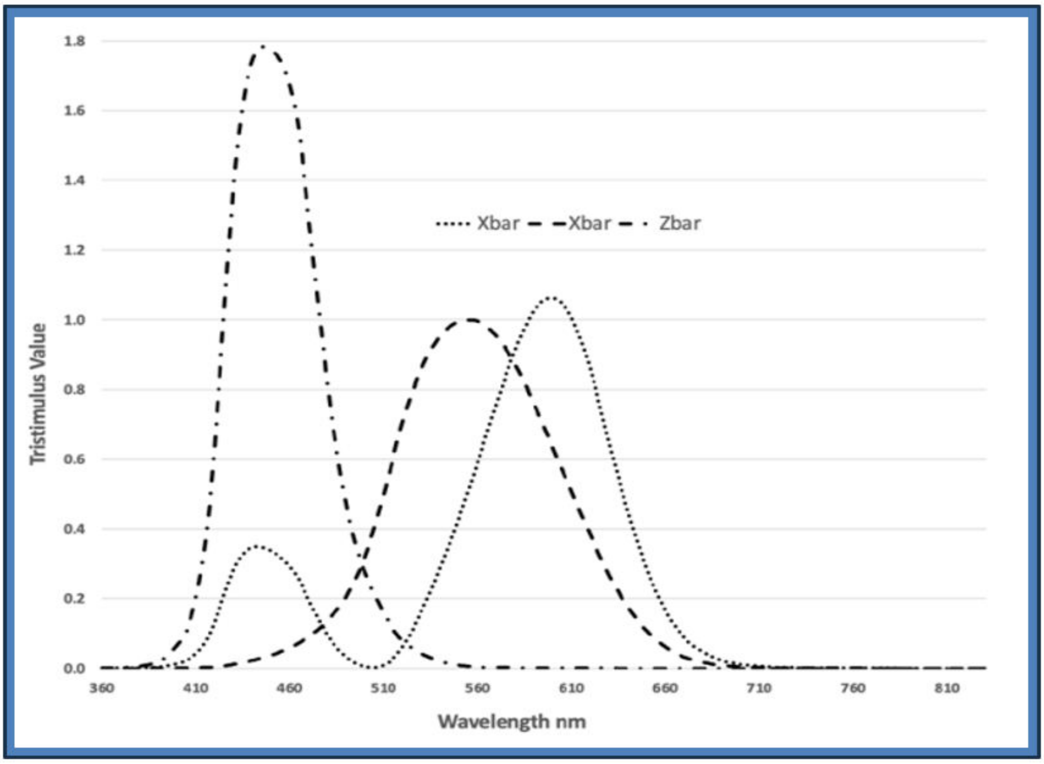

Figure-2. CIE 1931 2° XYZ color matching functions [1].

These cover a wide range of natural sunlight conditions, from overcast to bright midday sunlight. On the other hand, CCT ranges for different light sources may go down as low as 2000 K and up as high as 12500 K for cool, blueish light, according to open literature. Accurately measuring the perceived color of any light source is important in its representation of visual characteristics. Color appearance of light plays an important role both in research and practical lighting applications and usually is quantified by metrics like chromaticity coordinates and their correlated color temperature. Since the beginning of the 20th century, CCT has widely been applied within lighting research because of its simplicity as a one-dimensional metric and its importance in quantifying the light source's visual properties. CCT is a commonplace practice both within research and within lighting, but its accuracy is bound compared to more scientifically stringent methods reliant on heavy replication and validation. Historically, CCT has conventionally been used to describe the spectra of light sources in work related to lighting and color rendition. Older technologies, such as incandescent and gas discharge lamps-except for fluorescent lamps-had fairly stable spectral distributions; therefore, generalizations based on CCT were possible. However, with solid-state lighting allowing a wide range of spectral power distributions, the use of CCT as a sole measure of quality of light has been questioned and hence may not be fully or reliably representative of the color quality of a light source. This discussion presents computation, application, and limitations of CCT, and other approaches and complementary metrics to better characterize the color features of a light source are addressed. [9-12].

Today, The CCT has widely been used to quantify various light sources in different applications from architectural lighting to display systems. Light sources with lower CCTs, like 2700 K, tend to appear warm or yellowish-white in color, while higher CCTs, such as 6500 K, tend to appear cool or bluish-white in color. This categorization helps the user memorize an association between the CCT of a light source and its appearance, although intuitively it should be noted that higher temperatures would correspond to "cooler" colors, as from a mental perspective one associates the color blue with cool and red with warmth. Historically, incandescent sources were similar to blackbody radiators, and so CCT was adopted as a descriptor of light sources, defined by the temperature of the blackbody radiator that best approximates the color of the light. As temperature increases, the chromaticity coordinates of a blackbody describe a curved path on the chromaticity diagram termed the blackbody or Planckian locus. However, CCT cannot correctly depict colors that are far away from this curve because it considers only the yellow-blue axis and ignores other color changes. The widely accepted methodology for CCT calculation is to find the temperature where the iso-temperature line intersects the blackbody locus on the chromaticity diagram. Currently, the CIE recommends using iso-temperature lines which are perpendicular to the blackbody locus. While estimates of CCT and distribution temperature may be made experimentally, or by interpolation of chromaticity coordinates by eye, the use of computer methods is becoming increasingly more important in the direct computation of these quantities from spectral power distributions. [13-16].

Since irradiance in itself is a measure of the amount of light falling on a surface, we need to actually place this diffusing surface at the location where we want to measure the irradiance and then measure the light reflected off the diffuser [17]. The more the diffuser resembles a Lambertian surface, the better it reflects light. Part of the reflected light from the diffuser is directed, by means of a lens, through the input slit of the monochromator. Since the diffuser radiance is uniform there is no need to be critical about slight adjustments in lenses or monochromator position. Also, the radiance at any point is the result of light from all portions of the source. However, flat diffusers, like integrating spheres, are very susceptible to stray light problems, since any incident radiation is scattered in every direction, possibly entering the monochromator entrance.

In photometry, the comparator is the photometer. Since no photometer precisely duplicates the response curve of the human eye, we have to evaluate how well the photometer approximates this curve. The photometer integrates internally across the spectral range and delivers a single output value-a single numerical result. Most integrating photometers are calibrated using the CIE Illuminant A, a spectrally "smooth" light source similar to a blackbody radiator at 2856 K [17]. When a light source of other than CIE Illuminant A spectral distribution is measured by photometers, an error due to spectral mismatch of the photometer arises. This is corrected by a spectral mismatch correction factor, SMF, [18]. When a photometer measures a light source whose spectral power distribution is different from the one that was used for its calibration, there is a spectral mismatch error. For correction, the relative spectral responsivity of the photometer needs to be characterized; the formula, following calculates spectral mismatch correction factor, SMF: [17].

$$SMF = \frac{\int_{360}^{830nm} P_e^T(\lambda)\times V(\lambda)d\lambda \int_{all-wavelengths} P_e^S(\lambda)\times R(\lambda)d\lambda}{\int_{all-wavelengths} P_e^T(\lambda)\times R(\lambda)d\lambda \int_{360}^{830nm} P_e^S(\lambda)\times V(\lambda)d\lambda} \quad (11)$$

where

$P_e^T(\lambda)$: is the relative spectral output of the test source.

$P_e^S(\lambda)$: is the relative spectral output of the standard source.

$R(\lambda)$: is the relative spectral responsivity of the photometer.

$V(\lambda)$: is the spectral luminous efficiency function, which defines a photometric measurement.

This study aims to apply CCT curves and their equations for estimating uncertainty and variability in Spectral Measurement Factors (SMF) for a specific lamp. The accuracy of CCT curves is crucial, as variations in CCT can lead to significant uncertainties in SMF. The analysis revealed that the CCTs of standard lamps ranged from approximately 2400 K to 2750 K, while the test lamps showed a narrower range from 2043 K to 2095 K. These CCT differences contribute to the overall uncertainty in spectral measurements, as changes in CCT affect the spectral output relative to calibration standards. Therefore, accurately measuring these differences is essential for fine-tuning the SMF, ultimately enhancing the reliability of measurement systems.

2. EXPERIMENTS AND MEASUREMENTS

A setup using the NIS Spectroradiometer Ocean Optics HR 2000, which boasts a 4.7% uncertainty, was employed to measure the spectral power distribution of the NIS-Primary Standard and determine the spectral mismatch correction factor, as illustrated in Figure 3. The measurement process began by utilizing a photometric bench to capture the spectral power distribution directly. Light from the lamp was directed into the spectroradiometer’s entrance port via an optical fiber, ensuring that the light collected was representative of the source's output. The spectrum was then output through a USB port to a connected PC for data acquisition and subsequent analysis. To ensure accuracy and compliance, the Spectro radiometric measurement of light sources adhered to the CIE 63-1984 method recommended by the International Electrotechnical Commission (IEC) [19]. This method provides a standardized approach for evaluating the spectral characteristics of various light sources, which is essential for reliable calibration and comparison. Each lamp was carefully positioned half a meter above the spectroradiometer to maintain a consistent distance, thereby minimizing variability in the measurements. A fifteen-minute warm-up interval was observed for each lamp to stabilize the output before data recording commenced. This time frame allows for any fluctuations in light output to settle, ensuring that the measurements reflect the lamp's performance under steady-state conditions. The measurements were conducted in a temperature-controlled dark room

ISSN 1819-6608
ARPN Journal of Engineering and Applied Sciences

maintained at $(25 \pm 2)^0 C$, which is critical for reducing external influences on the spectral readings. This controlled environment minimizes the effects of ambient light and temperature variations, thus enhancing the reliability of the data collected. The combination of precise equipment, standardized methodologies, and controlled conditions contributes to the overall integrity of the spectral power distribution measurements, laying the groundwork for accurate analysis and further research in the field.

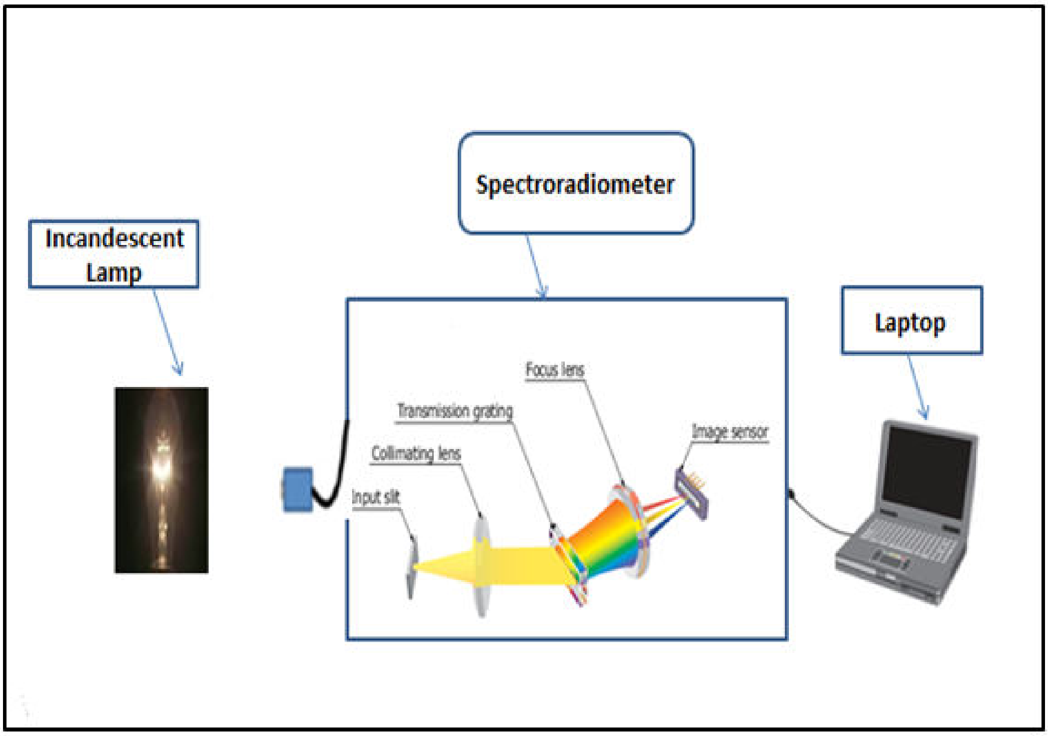

Figure-3. NIS setup for measuring the spectral power distribution.

Tables (1) and (2) are present the electrical control results for NIS standard lamps, which previously had been calibrated at the National Physical Laboratory - NPL (England). Very high accuracy calibration has been performed in NPL, only 0.8% uncertainty, hence, a good reference for many applications in photometry and colorimetry. These tables provide in detail certain key electrical parameters, including voltage, current, and power measurements, important in the performance and consistency assessment of these lamps. Apart from the standard lamps, tables present results also for six incandescent lamps in electrical control. Only these few lamps were chosen because their contribution to spectral mismatch correction factor calculation is vital for proper interpretation of spectral data. The selection of such incandescent lamps here allows for comparisons revealing how changes in electrical parameters may cause spectral outputs to change.

The tables also show the associated uncertainties of these measurements, which can yield information on the variability and reliability of these data. Understanding the uncertainty of these parameters is important for the correct calculation of the spectral mismatch correction factor, which would affect the precision of the spectral measurements taken from the setup. Combined with data from standard lamps of the NIS, tables like these form a rich database to evaluate the performance of the under-investigation light sources. These detailed data will help in developing more reliable calibration methods to enhance the overall accuracy in spectral power distribution measurements for better applications in lighting design, display technology, and color science.

VOL. 19, NO. 17, SEPTEMBER 2024 ISSN 1819-6608
ARPN Journal of Engineering and Applied Sciences

www.arpnjournals.com

Table-1. Results of electrical control for NIS standard lamps.

NIS Standard Lamps	SET Current (amperes)	Voltage (Volts)	Color temperature (Kelvin)	Total luminous flux (lumen)
NIS-E21	1.7869	102.1	2750	2587
NIS-E22	1.7991	101.6	2750	2597
NIS-E31	0.20482	91.9	2400	131.5
NIS-E32	0.20315	92.0	2400	130.8
NIS-E33	0.20382	92.4	2400	132.4

Table-2. Results of electrical control for tested lamps.

NIS Standard Lamps	SET Current (amperes)	Voltage (Volts)	Color temperature (Kelvin)	Total luminous flux (lumen)
NIS-1M-100	0.3050	116.9	2049	89
NIS-2M-100	0.3050	116.8	2043	89
NIS-1M-150	0.4551	114.9	2074	150
NIS-2M-150	0.4551	116.7	2054	164
NIS-1M-200	0.6050	116.7	2095	232
NIS-2M-200	0.6052	113.7	2070	225

3. RESULTS AND DISCUSSIONS

Figures Figures (4) to (9) present the measured SMF of each lamp at various CCTs. The fitted equations are given by Eqs. (12) to (17) can serve as predictive models to interpolate the SMF of each lamp for any value of CCT. These equations give the mathematical approach to how the spectral characteristics of the lamps interact with the calibration standards, in such a way that better adjustments can be done with regard to the variation in CCT. The spectral power distribution and CCT measurements through the system represented in Figure (3) give a wider approach to how these parameters are related by the lamps under test. It gives far better understanding of the impact of light quality and color temperature on performance and accuracy, while spectral measurements are in place. Tables (1) and (2) present in detail the result of electrical control of the NIS standard lamps calibrated in the National Physical Laboratory NPL-England, as well as the result of electrical control for six incandescent lamps. The tables provide essential data concerning some important electrical parameters (voltage, current, and power measurements) that form a basis for subsequent calculations related to the spectral mismatch correction factor. Using Equation, calculations have been conducted on measurements from these lamps to arrive at the spectral mismatch correction factor and the associated uncertainties for each lamp. This becomes an indispensable analysis for extracting the spectral output for each lamp concerning how well it fits to the calibration standards. The results of the spectral mismatch correction factors for incandescent lamps are represented in Figures (4) and (9) for a better pictorial understanding of the variation of these factors concerning different CCTs; the uncertainties associated with these measurements are systematically reflected in Tables (3) to (8).

ARPN Journal of Engineering and Applied Sciences

www.arpnjournals.com

SMF= 2E-05 CCT+ 0.9008 (12)

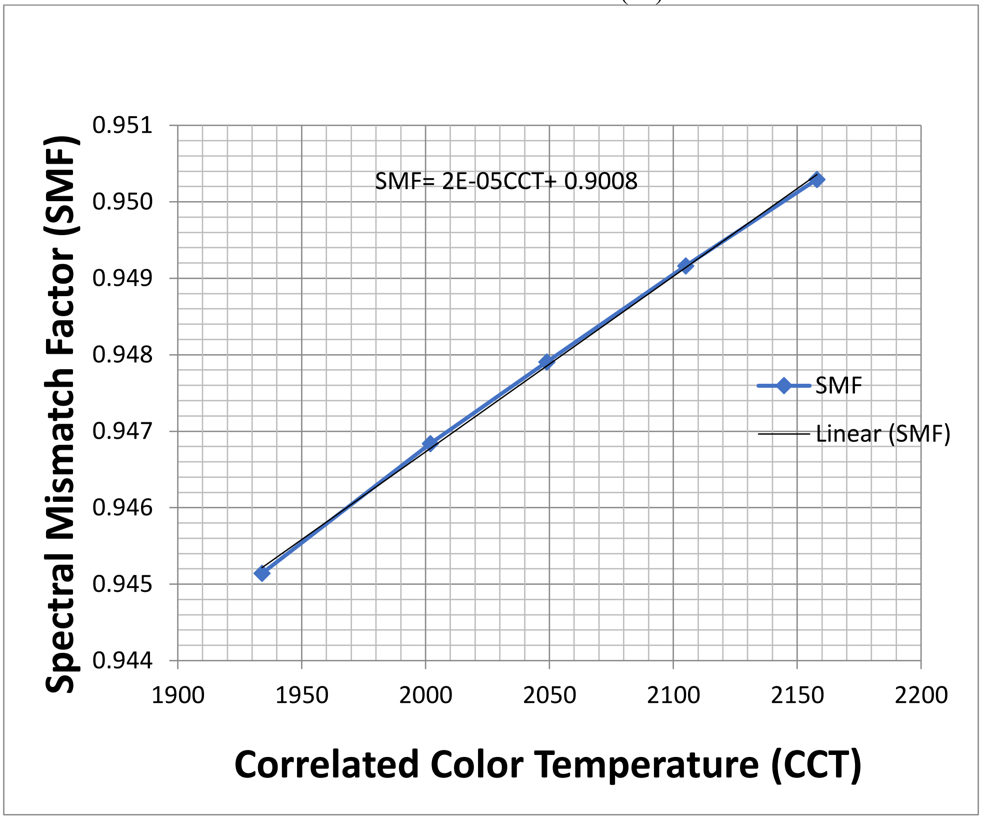

Figure-4. The spectral mismatch correction factors (SMF) against correlated color temperature (CCT) for the incandescent lamp NIS-M1-100.

SMF = 2E-05 CCT + 0.9009 (13)

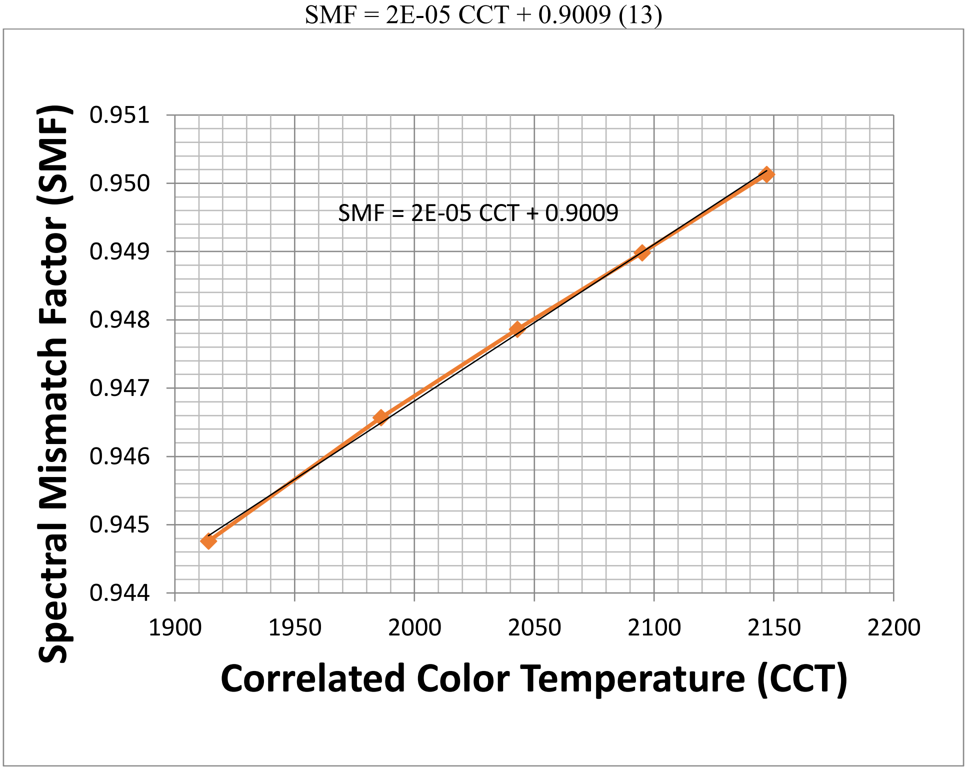

Figure-5. The spectral mismatch correction factors (SMF) against correlated color temperature (CCT) for the incandescent lamp NIS-M2-100.

ARPN Journal of Engineering and Applied Sciences

SMF = 2E-05 CCT + 0.8985 (14)

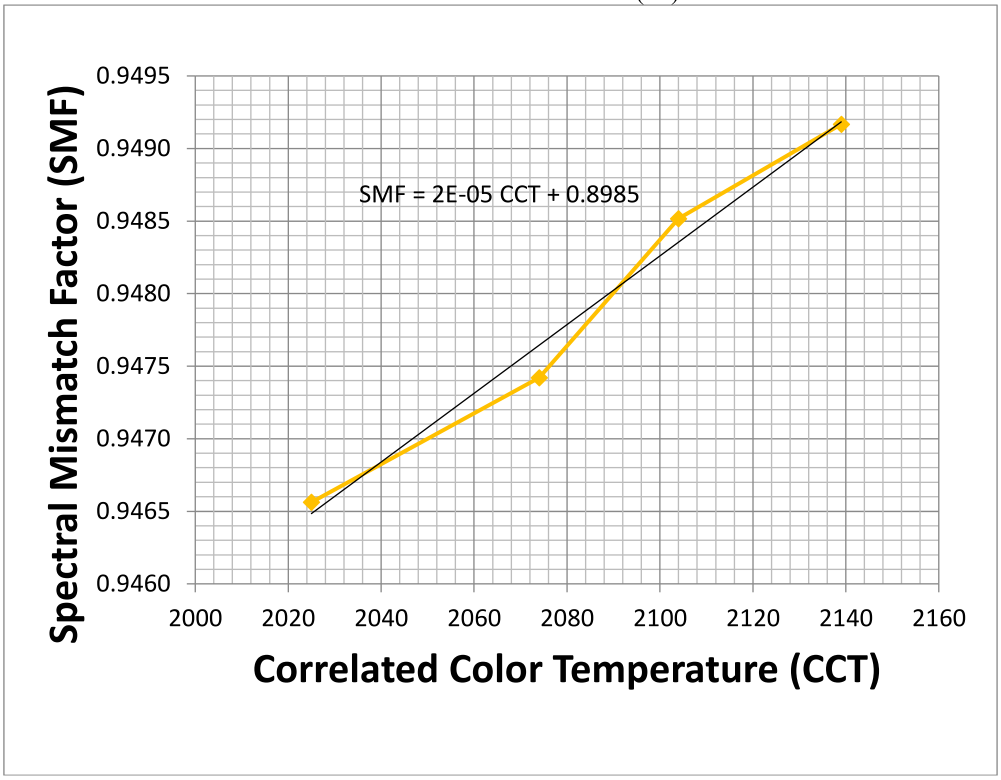

Figure-6. The spectral mismatch correction factors (SMF) against correlated color temperature (CCT) for the incandescent lamp NIS-M1-150.

SMF = 2E-05 CCT + 0.9015 (15)

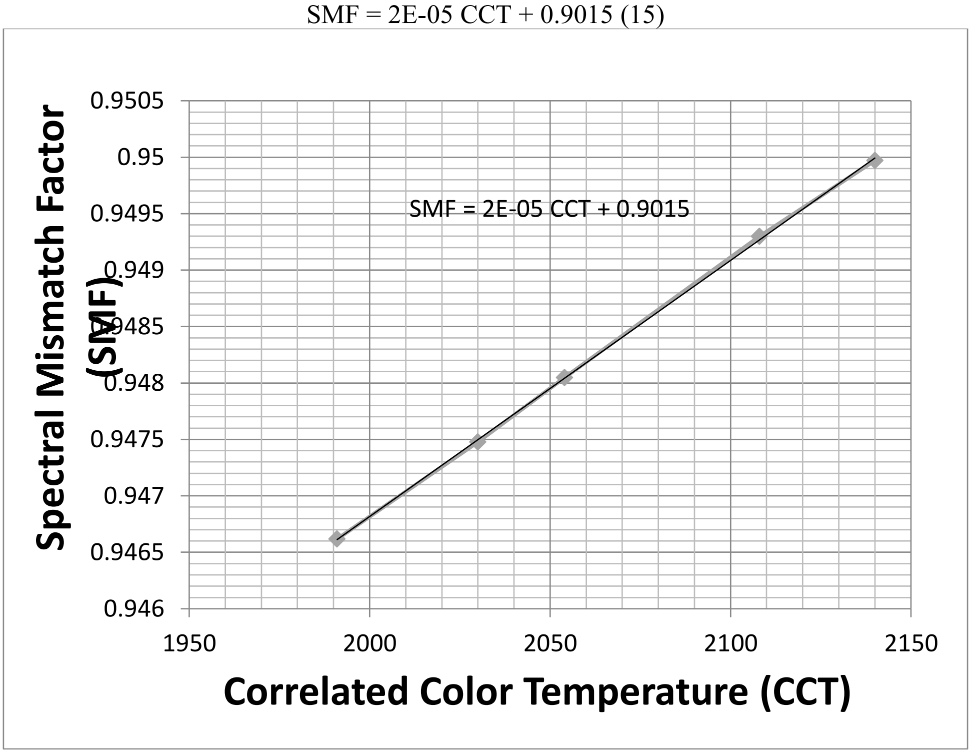

Figure-7. The spectral mismatch correction factors (SMF) against correlated color temperature (CCT) for the incandescent lamp NIS-M2-150.

SMF = 2E-05 CCT + 0.9012 (16)

ARPN Journal of Engineering and Applied Sciences

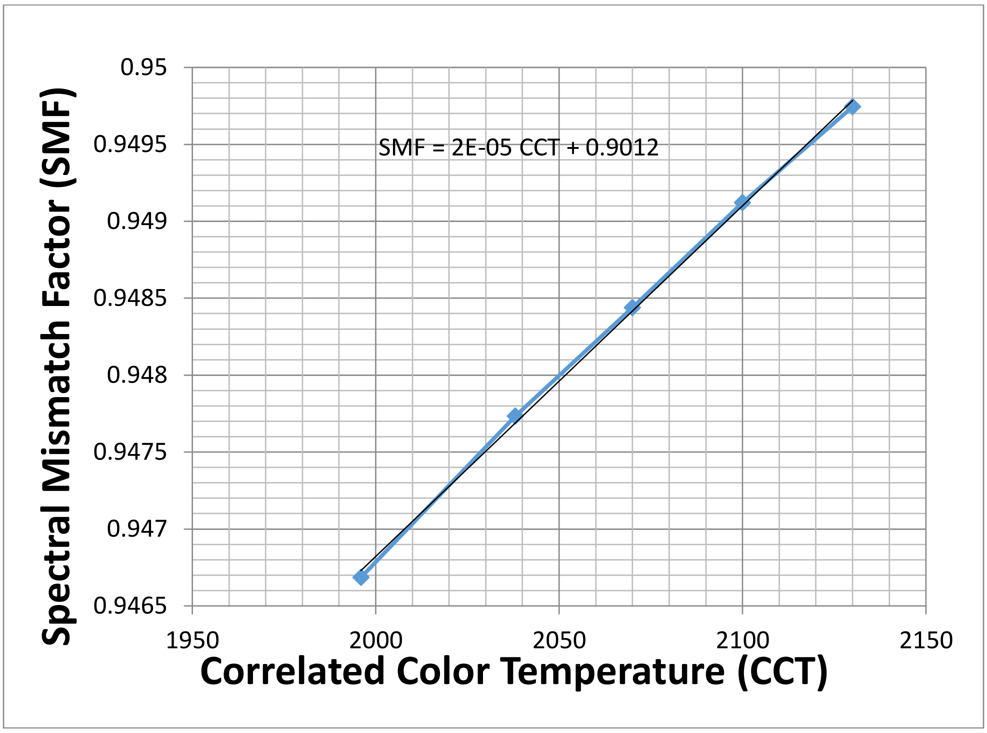

Figure-8. The spectral mismatch correction factors (SMF) against correlated color temperature (CCT) for the incandescent lamp NIS-M1-200.

SMF = 2E-05 CCT + 0.9013 (17)

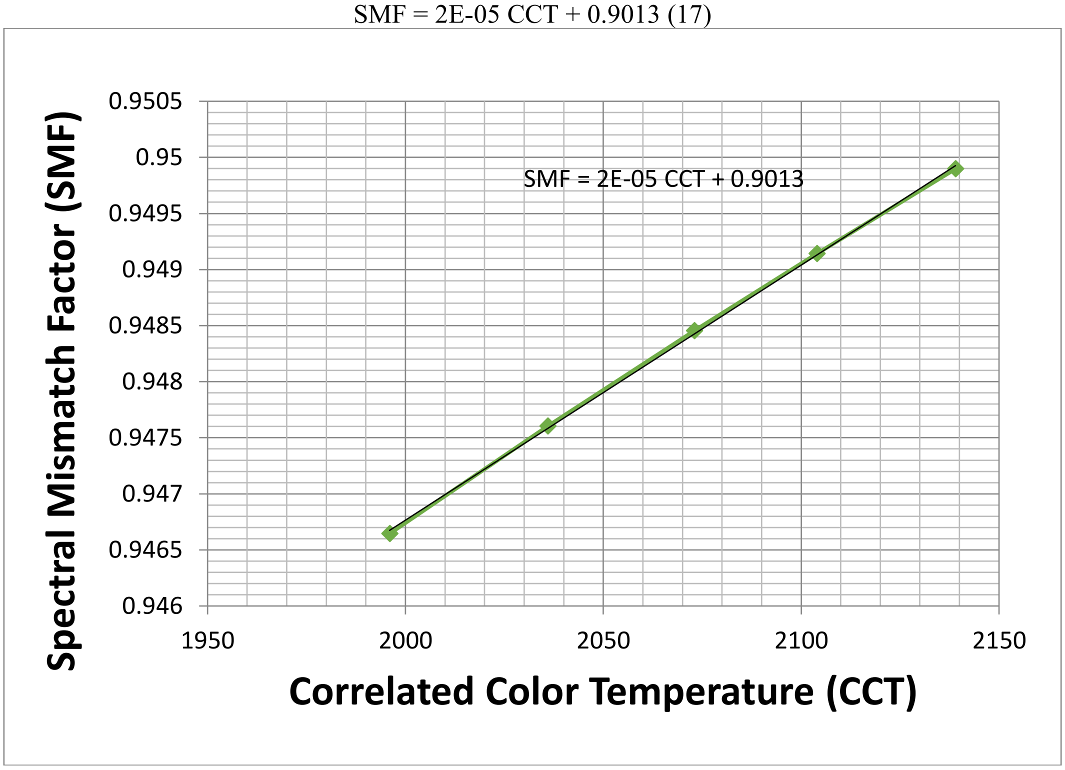

Figure-9. The spectral mismatch correction factors (SMF) against correlated color temperature (CCT) for the incandescent lamp NIS-M2-200.

4. UNCERTAINTY ANALYSIS

Giving the result of a measurement without a quantity describing the quality of the measurement result is quite indispensable so that the user of this information decides about the reliability of the result. Without such a statement, results of measurements cannot be compared or

ARPN Journal of Engineering and Applied Sciences

applied intelligently. Proper uncertainty evaluation will enhance trustworthiness and comparability of the measurements in many contexts. The best way of characterizing and stating measurement uncertainty should be universally applicable; that is, it should be applicable to all measurements whether the quantity being measured is unique or one member of a series, and whatever the nature of the input data. In this way uncertainty would be estimated under consistent, reproducible conditions in many different fields, from scientific research through to routine industrial testing and quality control. Several components may contribute to measurement uncertainty, conveniently categorized in two types depending on the method by which the numerical value of the component is estimated: Type A Uncertainty: This is evaluated by statistical methods. It is usually based on a sufficiently large number of repeated observations or measurements or based on statistical analysis of data (such as standard deviation, variance, or confidence intervals) that provide a quantitative estimate of the uncertainty. Type A uncertainty: The Type A evaluation is based on the inherent variability of the measurand; this may be due to random errors or fluctuations in the measurement process. Type B Uncertainty: On the other hand, Type B uncertainty is assessed by other means, which also can include a priori knowledge, experience, manufacturer specifications, or reference data from calibration reports. This category of uncertainty in general represents systematic errors, environmental conditions, or limitations in the measuring instrument. Unlike Type A, it does not rely on statistical sampling but instead uses documented information or expert judgment [20, 21].

By applying the law of propagation of uncertainty [22,23] as the following equation:
Hence, we have

$$u^2(SCF) = \delta^2 P_{iS}\left(\frac{\partial SCF}{\partial P_{iS}}\right)^2 + \delta^2 P_{it}\left(\frac{\partial SCF}{\partial P_{it}}\right)^2 + \delta^2 R_i\left(\frac{\partial SCF}{\partial R_i}\right)^2 \quad (18)$$

Where

P_{iS} : the summation of $P_e^S(\lambda)$ within the visible wavelength range.

P_{it} : the summation of $P_e^T(\lambda)$ within the visible wavelengths range.

R_i : the summation of $R(\lambda)$ within the visible wavelengths range.

Then from equation (2) we have

$$u(SCF) = \sqrt{\delta^2 P_{iS}\left(\frac{\partial SCF}{\partial P_{iS}}\right)^2 + \delta^2 P_{it}\left(\frac{\partial SCF}{\partial P_{it}}\right)^2 + \delta^2 R_i\left(\frac{\partial SCF}{\partial R_i}\right)^2} \quad (19)$$

The expanded uncertainty at a 95% confidence level, with a coverage factor of k=2, is a crucial metric in uncertainty reporting. This expanded uncertainty provides a wider margin of reliability, ensuring that there is a 95% probability that the true value lies within the specified range of the measured result. It is particularly important for high-precision measurements, where the consequences of error could significantly impact the outcome. In the case of the spectral mismatch correction factors, the uncertainty estimation varies depending on the correlated color temperature (CCT). As outlined in Tables (3) to (8), the uncertainty values range from 0.0011 to 0.0084. This variation is closely tied to the CCT, as different light sources emit spectra that can deviate from the calibration standards. Lower uncertainties are typically associated with light sources whose CCTs are more aligned with the calibration standards, while higher uncertainties arise when there is greater spectral deviation.

Table-3. Estimated Uncertainty correction factors (SMF) for the incandescent lamp NIS-M1-100.

NIS-M1-100	NIS-E21	NIS-E22	NIS-E24	NIS-E31	NIS-E32	NIS-E33
NIS-M1-100	0.0006	0.0014	0.0013	0.0084	0.0084	0.00847
NIS-M1-28-100	0.0015	0.0020	0.0019	0.0084	0.0084	0.00843
NIS-M1-29-100	0.0013	0.0018	0.0018	0.0084	0.0083	0.0084
NIS-M1-30-100	0.0012	0.0018	0.0017	0.0084	0.0084	0.0084
NIS-M1-31-100	0.0011	0.0017	0.0016	0.0084	0.0084	0.0084
NIS-M1-32-100	0.0010	0.0016	0.0015	0.0084	0.0083	0.0084

Table-4. Estimated Uncertainty correction factors (SMF) for the incandescent lamp NIS-M2-100.

NIS-M2-100	NIS-E21	NIS-E22	NIS-E24	NIS-E31	NIS-E32	NIS-E33
NIS-M2-28-100	0.0015	0.0083	0.0082	0.0153	0.0155	0.0153
NIS-M2-29-100	0.0014	0.0018	0.0018	0.0084	0.0083	0.0084
NIS-M2-30-100	0.0012	0.0017	0.0017	0.0084	0.0083	0.0084
NIS-M2-31-100	0.0011	0.0017	0.0016	0.0084	0.0083	0.0084
NIS-M2-32-100	0.0010	0.0016	0.0015	0.0084	0.0083	0.0084

ARPN Journal of Engineering and Applied Sciences

Table-5. Estimated Uncertainty correction factors (SMF) for the incandescent lamp NIS-M1-150.

NIS-M1-150	NIS-E21	NIS-E22	NIS-E24	NIS-E31	NIS-E32	NIS-E33
NIS-M1-43-150	0.0013	0.0018	0.0018	0.0084	0.0083	0.0084
NIS-M1-44-150	0.0013	0.0018	0.0017	0.0084	0.0083	0.0084
NIS-M1-45-150	0.0012	0.0017	0.0017	0.0084	0.0083	0.0084
NIS-M1-46-150	0.0011	0.0017	0.0016	0.0084	0.0083	0.0084
NIS-M1-47-150	0.0011	0.0016	0.0016	0.0084	0.0083	0.0084

Table-6. Estimated Uncertainty correction factors (SMF) for the incandescent lamp NIS-M2-150.

NIS-M2-150	NIS-E21	NIS-E22	NIS-E24	NIS-E31	NIS-E32	NIS-E33
NIS-M2-43-150	0.0013	0.0018	0.0018	0.0084	0.0083	0.0084
NIS-M2-44-150	0.0012	0.0018	0.0017	0.0084	0.0084	0.0084
NIS-M2-45-150	0.0012	0.0012	0.0017	0.0084	0.0084	0.0084
NIS-M2-46-150	0.0011	0.0017	0.0016	0.0084	0.0083	0.0084
NIS-M2-47-150	0.0010	0.0016	0.0016	0.0084	0.0083	0.0084

Table-7. Estimated Uncertainty correction factors (SMF) for the incandescent lamp NIS-M1-200.

NIS-M1-200	NIS-E21	NIS-E22	NIS-E24	NIS-E31	NIS-E32	NIS-E33
NIS-M1-58-200	0.0013	0.0018	0.0017	0.0084	0.0084	0.0084
NIS-M1-59-200	0.0012	0.0018	0.0017	0.0084	0.0083	0.0084
NIS-M1-60-200	0.0012	0.0017	0.0016	0.0084	0.0084	0.0084
NIS-M1-61-200	0.0011	0.0017	0.0016	0.0084	0.0083	0.0084
NIS-M1-62-200	0.0011	0.0016	0.0016	0.0084	0.0084	0.0084

Table-8. Estimated Uncertainty correction factors (SMF) for the incandescent lamp NIS-M2-200.

NIS-M2-200	NIS-E21	NIS-E22	NIS-E24	NIS-E31	NIS-E32	NIS-E33
NIS-M2-58-200	0.0013	0.0018	0.0017	0.0084	0.0084	0.0084
NIS-M2-59-200	0.0012	0.0017	0.0017	0.0084	0.0084	0.0084
NIS-M2-60-200	0.0011	0.0017	0.0016	0.0084	0.0084	0.0084
NIS-M2-61-200	0.0011	0.0017	0.0016	0.0084	0.0084	0.0084
NIS-M2-62-200	0.0010	0.0016	0.0016	0.0084	0.0084	0.0084

5. CONCLUSION

In this study, a comprehensive measurement setup in the test campaign consisted of the NIS Spectroradiometer Ocean Optics HR 2000 and a photometric bench. This spectroradiometer has an associated declared uncertainty of about 4.7%, and thus should yield precise measurements of a spectral nature, while the photometric bench provides a stable environment for ensuring that data collection is made with accuracy. Besides, a set of standard lamps for NIS total luminous flux previously calibrated at the National Physical Laboratory at England with an uncertainty of calibration of 0.8% was used so that all the measurements were well calibrated and would serve as a baseline for comparison. The setup was meant for measuring the CCT and the SPD of six incandescent lamps. The spectral distribution of the light emitted by the lamps was recorded by using a NIS Spectroradiometer Ocean Optics HR 2000. For each lamp, light was fed via an optical fiber into the entrance port of the spectrometer, which was connected to a PC through a USB port, providing readings in real time. This allowed the very precise measurement of the spectrum of light and hence allowed a more specific analysis of its SPD. The CCT curves with their respective equations provided the key in this analysis. These curves gave a great deal of information about how the SMF varies as a function of CCT for each lamp. Since SMF may be heavily responsible for influencing the accuracy of light measurement, understanding its shift for different values of CCT is paramount for improving general measurement precision. This was particularly important because the variations in CCT directly impacted the SMF, and errors in those measurements would flow into the final results. The CCT range for the standard lamps was from 2400 K to 2750 K, whereas for the test lamps, this was between 2043 and 2095 K. These differences in CCT for the standard and test lamps added to the variation in the SMF analyzed through the CCT curve and fitted equations depicted in Figures 4 to 9. These equations thus enabled the calculation of the SMF for each lamp at different CCTs, a very critical factor that has to do with how a large deviation occurs that might affect the accuracy of light measurement. Minimizing the SMF is quite essential in reducing the overall error of measurement, especially on total luminous flux measurements. The identified ways of achieving this included: the selection of standard lamps whose spectral characteristics are similar to those of the test lamps. This would minimize the spectral correction factor thereby giving accurate results. These were quantified and further elaborated with respect to possible fields of improvement in the reliability of measurement by tables of uncertainties given in Tables 3 and 8. Estimation of uncertainty for spectral mismatch correction factors depended upon CCT and hence lay between 0.0011 and 0.0084. Detailed breakdowns of variability for each lamp were given in Tables 3 through 8. Since uncertainty data was involved in constructing the uncertainty budget in detail, such an accurate uncertainty budget is meaningful in order to improve the total luminous flux measurements. In conclusion, precise calibration and stability of measurement conditions and further careful analysis of CCT and SMF are required in order to make the measurement errors and uncertainties as low as possible in this study. The combination of the configuration of NIS Spectroradiometer Ocean Optics HR 2000 coupled with the photometric bench and NPL-calibrated standard lamps was a perfect combination for accurate CCT and SPD of incandescent lamps, providing useful information on how to enhance the reliability of light measurements in diverse applications.

REFERENCES

[1] Peter R. Michael and *et al*. 2021. Correlated Color Temperature of AM0, AM1.5G, and AM1.5D Solar Irradiance with Applications to Photovoltaic Evaluation. IJISET - International Journal of Innovative Science, Engineering & Technology. 8(9).

[2] Rensselaer Polytechnic Institute, https://www.lrc.rpi.edu/programs/nlpip/lightinganswers/lightsources/whatisCCT.asp, last access 17 September 2021.

[3] Javier Hernández-Andres, *et al*. 1999. Calculating Correlated Color Temperatures Across the Entire Gamut of Daylight and Skylight Chromaticities, Applied Optics. 38(27).

[4] 931 2° CIE Standard Colorimetric Observer Data, https://www.rit.edu/cos/colorscience/rc_useful_data.php, last access 17 September 2021.

[5] 1931 CIE Chromaticity Diagram https://commons.wikimedia.org/wiki/File:PlanckianLocus.png, public domain by PARcommonswiki.

[6] C. S. McCamy. 1992. Correlated Color Temperature as an Explicit Function of Chromaticity Coordinates Color Research and Application. 17(2).

[7] Deane B. Judd, *et al*. 1964. Spectral Distribution of Typical Daylight as a Function of Correlated Color Temperature, Journal of the Optical Society of America. 54(8).

[8] Changjun Li, *et al*. 2016. Accurate Method for Computing Correlated Color Temperature, Optics Express. 24(13).

[9] Durmus D. 2021. Correlated color temperature: Use and limitations. Lighting Research & Technology. doi: 10.1177/14771535211034330.

[10] Hunt R. W. G., Pointer M. R. 2011. Measuring colour. 4th ed. West Sussex, UK: John Wiley & Sons.

[11] Davis R. A. 1931. Correlated color temperature for illuminants. Bureau of Standards Journal of Research. 7: 659.

[12] McCamy C. S. 1992. Correlated color temperature as an explicit function of chromaticity coordinates. Color Research and Application. 17(2): 142-144.

[13] Bennett C. A., Rey P. 1972. What's so hot about red? Human Factors, 14(2): 149-154. Wierzbicka A. The meaning of color terms: semantics, culture, and cognition. Cognitive Linguistics (includes Cognitive Linguistic Bibliography) 1990; 1(1): 99-150.

[14] R. Baribeau. 2007. CIE System of colorimetry. Photometry, Radiometry, and Colorimetry Course NRC, Ottawa, Canada.

[15] 2004. CIE, Publication No. 15:2004, Colorimetry 3rd ed., (Commission Internationale de l'Éclairage.

[16] R. Baribeau. 2007. CIE System of colorimetry. Photometry, Radiometry, and Colorimetry Course NRC, Ottawa, Canada.

ARPN Journal of Engineering and Applied Sciences

[17] A. A. Gaertner. 2007. Basics of Photometric Calibration. Photometry, Radiometry, and Colorimetry Course NRC, Ottawa, Canada.

[18] Ohno Y. 1996. Photometry Calibration. NIST Special Publication 250-37.

[19] 1984. International Electrotechnical Commission (IEC). Spectroradiometric measurement of light sources. Vienna: CIE Publication.

[20] 1995. International Organization for Standardization (ISO), Guide to the Expression of Uncertainty in Measurement.

[21] 1993. International Organization for Standardization (ISO), Guide to the Expression of Uncertainty in Measurement.

[22] Emma R. Woolliams. 2013. Determining the uncertainty associated with integrals of spectral quantities. Metrology for solid state lighting, EMRP-ENG05-1.3.1, Version 1.0.

[23] U. Krüger and G. Sauter. 2006. Comparison of methods for indicating the measurement uncertainty of integral parameters based on spectral data using the measurement uncertainty of the f1 value. Proceedings of the 2nd CIE Expert Symposium on Measurement Uncertainty, CIE x029: pp. 159-163.